Available online at www.sciencedirect.com
ScienceDirect
Trans. Nonferrous Met. Soc. China 30(2020) 3379−3389

Transactions of
Nonferrous Metals
Society of China
www.tnmsc.cn

Stability constants of Sb^{5+} with Cl^- and thermodynamics of $Sb-S-Cl-H_2O$ system involving complex behavior of Sb with Cl

Gang LI[1], Yun-tao XIN[1], Xiao-dong LÜ[1], Qing-hua TIAN[2], Kang YAN[3], Long-gang YE[4]

1. College of Materials Science and Engineering, Chongqing University, Chongqing 400044, China;
2. School of Metallurgy and Environment, Central South University, Changsha 410083, China;
3. School of Metallurgical Engineering, Jiangxi University of Science and Technology, Ganzhou 341000, China;
4. College of Metallurgy and Material Engineering, Hunan University of Technology, Zhuzhou 412007, China

Received 22 February 2020; accepted 27 September 2020

Abstract: The stability constants of Sb^{5+} with Cl^- as well as thermodynamics of the $Sb-S-Cl-H_2O$ system were calculated. The stability constants of Sb^{5+} with Cl^- were obtained by theoretical calculations of the absorbance of a Sb^{5+}-containing solution at different Cl^- concentrations, which was detected by spectrophotometric analysis at certain wavelengths of light (380 nm). The logarithmic values versus 10 of stability constants of Sb^{5+} with Cl^- were 1.795, 3.150, 4.191, 4.955, 5.427 and 5.511, respectively, and partly filled the data gaps in the hydrometallurgy of antimony. The presence and distribution of pentavalent antimony compounds under different conditions were analyzed based on equilibrium calculations. Thermodynamic equilibrium calculations were performed for $Sb-S-Cl-H_2O$ system, which included the complex behavior of Sb with Cl, and the equilibrium equations of related reactions in this system were integrated into the potential−pH diagram.

Key words: complex behavior; stability constant; thermodynamics; $Sb-S-Cl-H_2O$ system

1 Introduction

Antimony is widely used in various industrial fields in the form of alloys or compounds [1]. The most important compound of antimony is Sb_2O_3, which is mainly used as a flame retardant agent [2]. Most Sb_2O_3 products are produced by pyrometallurgy [3,4], while some are produced by hydrometallurgy, which involves the hydrolysis of a $SbCl_3$ solution obtained by acid leaching of antimony sulfides [5,6]. Some studies were reported on the hydrometallurgy of antimony in an alkaline system, while a few studies were reported in acid solution [7,8]. The antimony ions could not stabilize independently in solution, and hence, the concentration of antimony would be very low, unless the antimony ions were converted into stable species [9]. Generally, antimony needs to be maintained in stable form, as (thio)antimonite/(thio) antimonite [10,11] in alkaline solution and antimony complexes in acid solution [1,12]. The thermodynamic data of antimony complexes are different from those of antimony ions, and the Gibbs free energies (or equilibrium constants) of related reactions are also different. The standard redox potential of $SbCl_3/Sb$ is lower than that of Sb^{3+}/Sb, and the pH required for hydrolysis of $SbCl_3$ with H_2O is higher than that of Sb^{3+} with H_2O. However, antimony complexes are not considered in thermodynamic studies, which leads to misunderstanding of the hydrometallurgical process

---

Foundation item: Projects (51904048, 51922108) supported by the National Natural Science Foundation of China; Project (2019JJ20031) supported by the Hunan Natural Science Foundation, China; Project (gjj170507) supported by the Scientific Research Foundation of Jiangxi Provincial Department of Education, China

Corresponding author: Yun-tao XIN, Tel: +86-18580090137, E-mail: xinyuntao@cqu.edu.cn;
Qing-hua TIAN, Tel: +86-731-88877863, E-mail: qinghua@csu.edu.cn

DOI: 10.1016/S1003-6326(20)65469-3

of antimony. Therefore, it is important to modify such thermodynamic studies by considering the complex behavior of antimony with chlorine. There are two aspects of the complex behavior of antimony, namely, Sb^{3+} with Cl^- and Sb^{5+} with Cl^-. The complex reactions between antimony and chlorine are listed [13]:

$$Sb^{3+}+iCl^-=SbCl_i^{(3-i)},\ \beta'_i=[SbCl_i^{(3-i)}]/[Sb^{3+}][Cl^-]^i \quad (1)$$

$$Sb^{5+}+iCl^-=SbCl_i^{(5-i)},\ \beta_i=[SbCl_i^{(5-i)}]/[Sb^{5+}][Cl^-]^i \quad (2)$$

where β'_i is the stability constant of Sb^{3+} with Cl^-, the 10-based logarithms for which are 2.26, 3.49, 4.18, 4.72, 4.70 and 4.10, respectively [1,14], and β_i is the stability constant of Sb^{5+} with Cl^-, which is unknown.

There are comprehensive studies on the complex behavior of Sb^{3+} with Cl^- [14]. A theoretical study of the Sb^{3+}−OH^-−Cl^- system, which is based on the complex behavior of Sb^{3+} with Cl^-, was carried out in our previous study [15]. The presence and distributions of Sb^{3+} complexes under different conditions were analyzed by thermodynamic calculations. Theoretic calculations and verified experiments revealed that the hydrolysis reaction of $SbCl_3$ complexes produced $Sb_4O_5Cl_2$ but not SbOCl, which was different from our default understanding [1,16,17]. Thermodynamic studies such as potential−pH diagrams do not take $Sb_4O_5Cl_2$ into account [18,19], and the results of the thermodynamic calculations are different from the reality. Therefore, this inconsistency must be addressed to gain a better understanding of antimony-containing solution.

A thermodynamic study based on the complex behavior of Sb^{5+} with Cl^- is absent, due to the absence of the stability constants of Sb^{5+} with Cl^- and the loss of some thermodynamic data of the pentavalent antimony ions. The presence and distributions of Sb^{5+} complexes under different conditions are still unclear. However, some Sb^{5+} ions can exist in acidic solutions during the oxidation leaching of antimony sulfides in acid solution, and they can form complexes with ligands [20−22]. The reaction thermodynamics conditions for these complexes are different from those for Sb^{5+}, and it is difficult to determine the production conditions in the hydrometallurgy of antimony without a systematic thermodynamic study. Therefore, it is necessary to study its complex behavior and obtain the stability constants of Sb^{5+} with Cl^-. Then, the thermodynamic data can be obtained by determining its complex behavior, and the thermodynamic study of antimony can be further modified.

In this study, thermodynamic study of the Sb−S−Cl−H_2O system was carried out by considering the complex behavior of Sb with Cl^-. The stability constants of Sb^{5+} with Cl^- were obtained using the spectrophotometric method, and thermodynamic equilibrium calculations were developed by considering the complex behavior of antimony with chlorine. Then, equilibrium equations of related reactions in the thermodynamic study of the Sb−S−Cl−H_2O system were obtained and systematically integrated into a potential−pH diagram.

2 Experiment and theoretical calculation

2.1 Spectrophotometric experiments

The stability constants of Sb^{5+} with Cl^- were obtained by using the spectrophotometric method [23]. The Sb^{5+}-containing solution was prepared by oxidation-leaching of Sb_2O_3 (AR, Sinopharm Chemical Reagent Co., Ltd.) in sulfuric acid (AR, Sinopharm Chemical Reagent Co., Ltd.) with an oxidant of ozone-containing gas, which was generated by an ozone generator (OZOMJB−80B, ANQIU OZOMAX, China). The pH value of the solution was kept at approximately 1.0 and the potential of the solution was maintained above 0.9 V by oxidation of the ozone-containing gas, which was measured by using a pH/mV meter (PHS−3E, Inesa, Analytical Instrument Co., Ltd.), allowing the antimony(III) to be completely oxidized into antimony(V) [19]. The oxidation process was performed in a water bath at 25 °C. When the potential of the solution was stable, the oxidation process was complete, and the solution was immediately sent for detection, as shown in Fig. 1.

The oxygen used in this study was of industrial grade, and the ozone content was 7 wt.%. The Cl^- ligand was added in the form of a NaCl powder (AR, Sinopharm Chemical Reagent Co., Ltd.). The purities of the chemicals are given in Table 1.

The concentrations of antimony and chlorine in solutions were determined by an inductively coupled plasma atomic emission spectroscopy (ICP-AES, PS−6, Baird, USA). The absorbance of the solutions with different concentrations of antimony and chlorine were detected by a spectrophotometer (721, INESA, Inesa, Analytical Instrument Co., Ltd.) under certain wavelengths of light, and the stability constants were calculated using the methods described in Section 2.2. The path length of the cuvette (Quartz Cells, Changzhou Putian Instrument Manufacturing Co., Ltd.), or the thickness of the solution, was 1.0 cm. The light path and optical system of the spectrophotometer are shown in Fig. 2.

The absorbance of the solutions was detected at 25 °C in the thermostatic chamber, and the system was operated at atmospheric pressure. The structure of the sulfate radical makes it hard to establish a relationship with cations compared to that of the chloridion, so it is reasonable to take no account of the interactions between sulfates and antimony ions in this study.

2.2 Theoretical calculations of stability constants

Thermodynamic calculations were based on the following assumptions [23,24]: (1) The system was operated at 25 °C and under atmospheric

Table 1 Purities of chemicals

Component	Supplier	Mass fraction	Application
Sb_2O_3	Sinopharm Chemical Reagent Co., Ltd.	≥0.990	Provide antimony
H_2SO_4	Sinopharm Chemical Reagent Co., Ltd.	≥0.980	Prepare acid solution
NaCl	Sinopharm Chemical Reagent Co., Ltd.	≥0.995	Provide ligands
O_2	RUIXIN Gas Co., Ltd.	≥0.9999	Act as material for oxidant

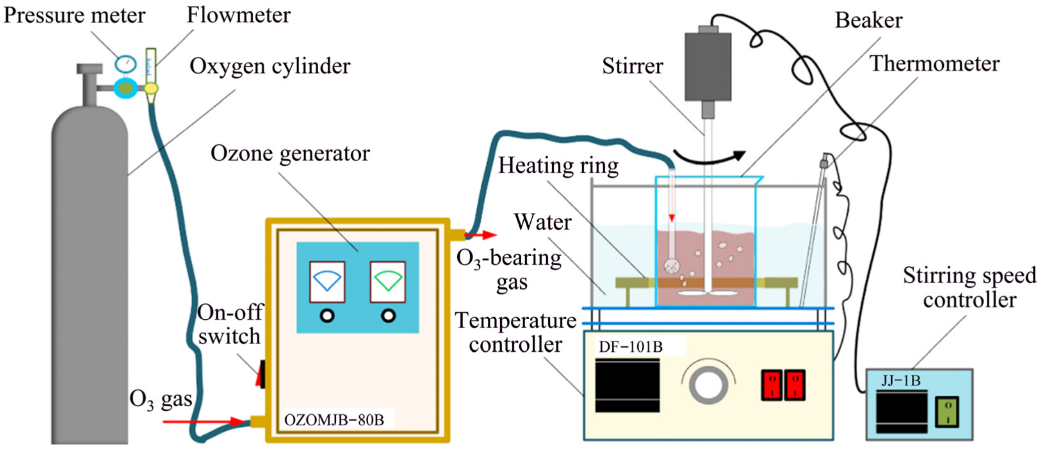

Fig. 1 Apparatus used for preparation of Sb^{5+}-bearing solution

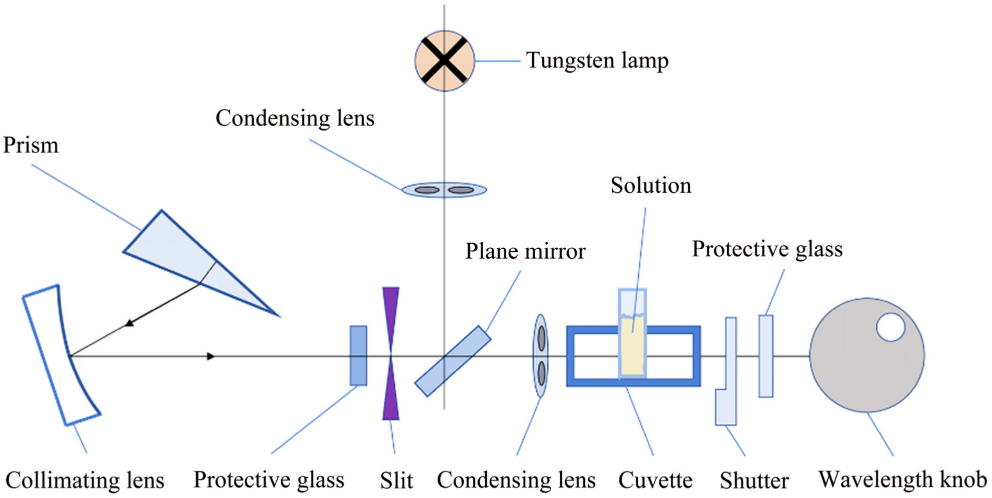

Fig. 2 Light path and optical system of 721 model spectrophotometer

pressure; (2) The thermal effects of system reactions were not considered; (3) The activity coefficient equaled 1.0 and was not affected by ionic strength or the solution system; (4) The system was in a state of equilibrium; (5) No gas and other unexpected materials were generated.

According to the Lambert−beer law [25], the absorbance of a solution with a certain thickness under certain wavelengths of light can be demonstrated according to Eq. (3):

$$\lg(I_0/I)=D=\varepsilon_0[\mathrm{M}]l \tag{3}$$

where I_0 and I stand for the intensities of the incident and emergent light, respectively, D stands for the absorbance of the solution, ε_0 is the extinction coefficient of metal compounds, l is the thickness of the solution, and [M] stands for the concentration of metal compounds in the solution. If the ligands and other ions have no influence on the incident light, the absorbance of the solution can be obtained by Eq. (4). In this study, the pH value of the solution was acidic and maintained at approximately 1.0, where few $\mathrm{SbO_3^-}$ existed, as well as $\mathrm{HSbO_3}$ and other pentavalent antimony compounds. Thus, the influence of $\mathrm{SbO_3^-}$, $\mathrm{HSbO_3}$ and other pentavalent antimony compounds on absorbance was not considered here, which could be verified after the stability constants were obtained.

$$D=(\varepsilon_0[\mathrm{Sb^{5+}}]+\varepsilon_1[\mathrm{SbCl^{4+}}]+\varepsilon_i[\mathrm{SbCl}_i^{(5-i)}])/l \tag{4}$$

The ε_m is used as the mean extinction coefficient of metal ions and complexes, and thus

$$D=\varepsilon_\mathrm{m}T_\mathrm{M}l \tag{5}$$

The number of ligands (i in Eq. (1) or Eq. (2)) is related to the valence and radius of the central ion, corresponding to the acting force between the central ion and ligands and space for ligands. Although the valence of the $\mathrm{Sb^{5+}}$ ion is higher than that of the $\mathrm{Sb^{3+}}$ ion, the radius (or space for ligands) of the $\mathrm{Sb^{5+}}$ ion is smaller than that of the $\mathrm{Sb^{3+}}$ ion, and the number of ligands (i) is six by comprehensive consideration. Thus, there exist $\mathrm{SbCl^{4+}}$, $\mathrm{SbCl_2^{3+}}$, $\mathrm{SbCl_3^{2+}}$, $\mathrm{SbCl_4^{+}}$, $\mathrm{SbCl_5}$ and $\mathrm{SbCl_6^{-}}$ complexes in the solution, the extinction coefficients of which are ε_1, ε_2, ε_3, ε_4, ε_5 and ε_6, respectively. The $\mathrm{Sb^{5+}}$ ions and $\mathrm{Cl^-}$ ions are coordinated together and form different complexes, as shown in Fig. 3. The distributions of SbCl_i^{5-i} complexes are determined by pH, stability constants, and other conditions.

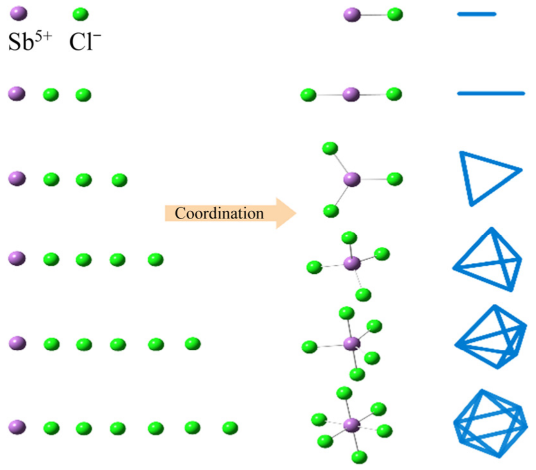

Fig. 3 Coordination processes between $\mathrm{Sb^{5+}}$ and $\mathrm{Cl^-}$

The T_M, T_L and $\bar{n}$ are used to describe total metal ions, total ligands, and the mean complexing number, respectively:

$$T_\mathrm{M}=[\mathrm{Sb^{5+}}]+[\mathrm{SbCl^{4+}}]+[\mathrm{SbCl_2^{3+}}]+[\mathrm{SbCl_3^{2+}}]+[\mathrm{SbCl_4^{+}}]+[\mathrm{SbCl_5}]+[\mathrm{SbCl_6^{-}}] \tag{6}$$

$$T_\mathrm{L}=[\mathrm{Cl^-}]+[\mathrm{SbCl^{4+}}]+2[\mathrm{SbCl_2^{3+}}]+3[\mathrm{SbCl_3^{2+}}]+4[\mathrm{SbCl_4^{+}}]+5[\mathrm{SbCl_5}]+6[\mathrm{SbCl_6^{-}}] \tag{7}$$

$$\begin{aligned}\bar{n}&=([\mathrm{SbCl^{4+}}]+2[\mathrm{SbCl_2^{3+}}]+3[\mathrm{SbCl_3^{2+}}]+4[\mathrm{SbCl_4^{+}}]+5[\mathrm{SbCl_5}]+6[\mathrm{SbCl_6^{-}}])/T_\mathrm{M}\\&=(\beta_1[\mathrm{Cl^-}]+2\beta_2[\mathrm{Cl^-}]^2+3\beta_3[\mathrm{Cl^-}]^3+4\beta_4[\mathrm{Cl^-}]^4+5\beta_5[\mathrm{Cl^-}]^5+6\beta_6[\mathrm{Cl^-}]^6)/(1+\beta_1[\mathrm{Cl^-}]+\beta_2[\mathrm{Cl^-}]^2+\beta_3[\mathrm{Cl^-}]^3+\beta_4[\mathrm{Cl^-}]^4+\beta_5[\mathrm{Cl^-}]^5+\beta_6[\mathrm{Cl^-}]^6)\\&=(T_\mathrm{L}-[\mathrm{Cl^-}])/T_\mathrm{M}\end{aligned} \tag{8}$$

Based on Eqs. (2)−(8), ε_m could be obtained:

$$\begin{aligned}\varepsilon_\mathrm{m}&=D/\mathrm{T_M}l\\&=(\varepsilon_0+\varepsilon_1\beta_1[\mathrm{Cl^-}]+\varepsilon_2\beta_2[\mathrm{Cl^-}]^2+\varepsilon_3\beta_3[\mathrm{Cl^-}]^3+\varepsilon_4\beta_4[\mathrm{Cl^-}]^4+\varepsilon_5\beta_5[\mathrm{Cl^-}]^5+\varepsilon_6\beta_6[\mathrm{Cl^-}]^6)/(1+\beta_1[\mathrm{Cl^-}]+\beta_2[\mathrm{Cl^-}]^2+\beta_3[\mathrm{Cl^-}]^3+\beta_4[\mathrm{Cl^-}]^4+\beta_5[\mathrm{Cl^-}]^5+\beta_6[\mathrm{Cl^-}]^6)\end{aligned} \tag{9}$$

It is easily seen that ε_m (or D) and $\bar{n}$ are functions of concentration of the ligand $\mathrm{Cl^-}$. When the concentration of ligand $\mathrm{Cl^-}$ is fixed, ε_m (or D) could be obtained. For a series of solutions with different T_M (T_M1, T_M2, $T_{\mathrm{M}i}$, ⋯) and T_L (T_L1, T_L2, $T_{\mathrm{L}i}$, ⋯), when ε_m (or D) is constant, the free ligand $[\mathrm{Cl^-}]$ in the solution should be the same, as well as $\bar{n}$:

$$(T_\mathrm{L1}-[\mathrm{Cl^-}])/T_\mathrm{M1}=(T_\mathrm{L2}-[\mathrm{Cl^-}])/T_\mathrm{M2}=\cdots=(T_{\mathrm{L}i}-[\mathrm{Cl^-}])/T_{\mathrm{M}i}=\bar{n} \tag{10}$$

Each $T_{\mathrm{M}i}$ and $T_{\mathrm{L}i}$ pair was obtained under a certain ε_m (or D). Then, T_M was plotted versus T_L

and a straight line could be obtained using Eq. (11). If the plot of T_M versus T_L is not a straight line, it means that polynuclear complexes exist in the solution.

$$T_L=\bar{n}\,T_M+[\mathrm{Cl}^-] \quad (11)$$

The slope of the line stands for $\bar{n}$, and the intercept stands for $[\mathrm{Cl}^-]$. Afterwards, the stability constants β_i can be calculated by using a multivariate Eq. (8).

2.3 Thermodynamic calculations and potential−pH diagram

Thermodynamic study could provide theoretical guidance for antimony metallurgy analysis and applications. Owing to the interactions between antimony and chlorine, a thermodynamic study is inadequate and needs to be modified. The thermodynamic equilibrium calculation of antimony in solution was launched by the equilibrium calculation of the complex behavior of Sb^{5+} with Cl^-. The reactions in the Sb−S−Cl−H_2O system would be calculated based on the principle of charge and mass balance. Every equilibrium reaction would thus be a function of the redox potential and pH. Three different situations in the thermodynamic study are listed below [26].

(1) Reactions with H^+ and without electronic transfer:

$$a\mathrm{A}+n\mathrm{H}^+=b\mathrm{B}+c\mathrm{H_2O} \quad (12)$$

$$\mathrm{pH}=-\Delta_r G_m^{\ominus}/(2.303nRT)-\lg(a_B^b/a_A^a)/n$$

where $\Delta_r G_m^{\ominus}$ is Gibbs free energy of Reaction (12), R is gas constant, namely 8.314 J/(mol·K), T is the temperature, a_A and a_B are the activities of reactant A and product B.

(2) Reactions with electronic transfer and without H^+:

$$a\mathrm{A}+ze=b\mathrm{B} \quad (13)$$

$$\varphi=-\Delta_r G_m^{\ominus}/(zF)-0.0591\lg(a_B^b/a_A^a)/z$$

where F is faraday constant.

(3) Reactions with H^+ and electronic transfer:

$$a\mathrm{A}+n\mathrm{H}^++ze=b\mathrm{B}+c\mathrm{H_2O} \quad (14)$$

$$\varphi=-\Delta_r G_m^{\ominus}/(zF)-0.0591\lg(a_B^b/a_A^a)/z-0.0591n\mathrm{pH}/z$$

When equilibrium equations were integrated into a potential−pH diagram, these thermodynamic reactions in the Sb−S−Cl−H_2O system could be intuitive and systematical.

3 Results and discussion

3.1 Wavelength of light

The wavelength of light should be chosen first in the spectrophotometry experiment. The absorbance of $\mathrm{SbCl_5}$ under different wavelengths of light was studied using quantum chemistry calculations with Gaussian software. The density functional theory (DFT) [27] at the B3LYP level with DGDZVP as the basis set was carried out to study the Uv−Vis absorption spectrum of $\mathrm{SbCl_5}$ in water, as seen in Fig. 4. At the same time, the verification test on the absorbance of $\mathrm{SbCl_5}$ solution (0.05 mol/L Sb^{5+} with 0.25 mol/L Cl^- in sulfuric acid solution) was carried out at different wavelengths in the range of 300−700 nm, and the results are shown in Fig. 4.

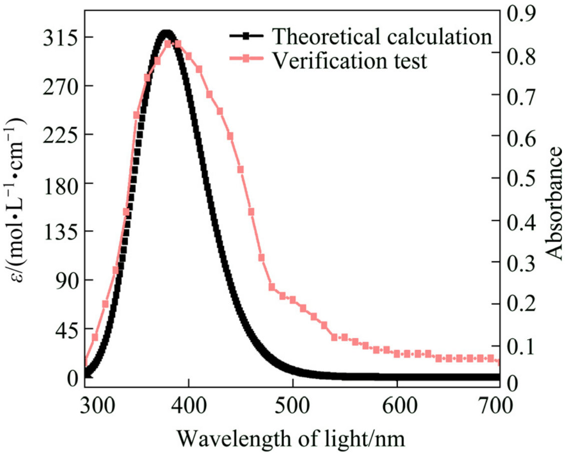

Fig. 4 Absorption curves of $\mathrm{SbCl_5}$ in theoretic calculation and verification test

As observed in Fig. 4, the peak of the curve was on the 380 nm light in the theoretic calculations, so the absorbance of the $\mathrm{SbCl_5}$ solution would be the maximum on the 380 nm light. The same conclusion was reached from the verification test. To guarantee the accuracy of this study, the wavelength of light was chosen as 380 nm. The Cl^- ligand was added in the form of sodium chloride, which is a kind of strong electrolyte, so there were equal concentrations of sodium ions and chloridions in the solution. The assumption was made that the sodium ion has no effect on the absorbance of the solution in this study.

3.2 Stability constants of Sb^{5+} with Cl^-

The I of the solution with different

concentrations of Sb^{5+} and Cl^- was detected. Then, D and ε_m were calculated by using Eq. (3), and the results of ε_m are listed in Table 2 while the plots versus $[Cl^-]_T$ with different $[Sb^{5+}]_T$ are shown in Fig. 5.

By fitting the data in Fig. 5, a fitted straight line was obtained and the parameters of the line were determined using Eqs. (15)−(17):

$$y=9.21511x+6.70538,\ [Sb^{5+}]_T=0.02345\ \text{mol/L},\ R^2=0.95291,\ D_0=0.157241161 \tag{15}$$

$$y=9.41905x+4.37793,\ [Sb^{5+}]_T=0.04501\ \text{mol/L},\ R^2=0.97039,\ D_0=0.197050629 \tag{16}$$

$$y=9.00882x+2.45486,\ [Sb^{5+}]_T=0.08576\ \text{mol/L},\ R^2=0.93657,\ D_0=0.171251034 \tag{17}$$

Table 2 Results of I detected by spectrophotometer and D and ε_m by calculation

No.	$[Sb^{5+}]_T$/ $(mol \cdot L^{-1})$	$[Cl^-]_T$/ $(mol \cdot L^{-1})$	D	ε_m/ $(mol \cdot L^{-1} \cdot cm^{-1})$
1	0.02345	0.02949	0.16241	6.92587
2	0.02345	0.09229	0.17587	7.49996
3	0.02345	0.13800	0.19179	8.17864
4	0.02345	0.22397	0.20343	8.67487
5	0.04501	0.09773	0.23284	5.17316
6	0.04501	0.19523	0.28400	6.30963
7	0.04501	0.29286	0.32975	7.32624
8	0.04501	0.3906	0.35556	7.89961
9	0.08576	0.26892	0.33630	4.82080
10	0.08576	0.35732	0.40894	5.86203
11	0.08576	0.48608	0.45469	6.51796
12	0.08576	0.55065	0.53018	7.60003

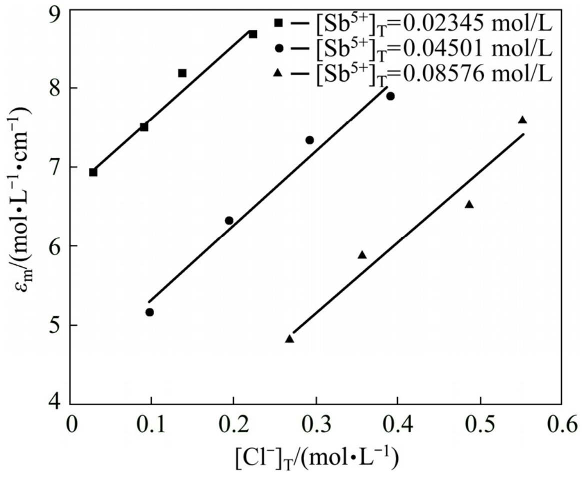

Fig. 5 ε_m versus $[Cl^-]_T$ with different $[Sb^{5+}]_T$

From the results of fitted lines, the Adj. R^2 values were 0.95291, 0.97039 and 0.93657, respectively, which means that the lines fit well with the data. The intercepts of the lines represented the ε_m of metal ions without ligands, namely ε_{01}, ε_{02} and ε_{03}; D_0 indicated the absorbance of Sb^{5+} without Cl^-, namely D_{01}, D_{02} and D_{03}. With the increase of Sb^{5+} concentration, the absorbance of Sb^{5+} without Cl^- fluctuated in a narrow range. The standard deviation (SD) of D_0 was 0.0202, which was relatively small, indicating that the Sb^{5+} ions have little effect on the absorbance of Sb^{5+} and Cl^-. For there are six β in the system, six ε values of equal difference were chosen. Each ε could find three points in the three fitted lines, and each group of the three points could form a straight line, as listed in Eq. (11) and shown in Fig. 6. It can be seen that there were two negative values of $[Cl^-]_T$ in Fig. 6, although it is impossible for this to be realized in reality, as it is common and normal in the mathematical model.

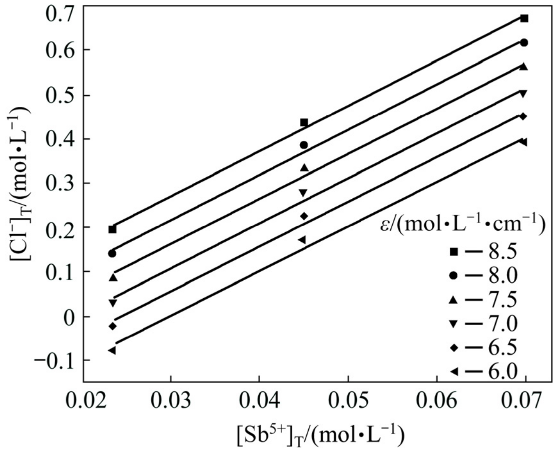

Fig. 6 $[Cl^-]_T$ versus $[Sb^{5+}]_T$ at different ε

From Fig. 6, it can be easily seen that the six straight lines had almost the same slope, and the differences were due to the differences in the stability constants β_i of the complexes, which would lead to different complex concentrations. The straight lines also indicated that there were no polynuclear complexes in the solution, and the stability constants β_i could be obtained using the method introduced previously. The six equations are listed below:

$$y=\overline{n}_1 x+[Cl^-]_1=10.26360x-0.03841,\ R^2=0.99475 \tag{18}$$

$$y=\overline{n}_2 x+[Cl^-]_2=10.23504x-0.09138,\ R^2=0.99381 \tag{19}$$

$$y=\bar{n}_3x+[\mathrm{Cl}^-]_3=10.20647x-0.14434,\ R^2=0.99279 \quad (20)$$

$$y=\bar{n}_4x+[\mathrm{Cl}^-]_4=10.17791x-0.19731,\ R^2=0.99169 \quad (21)$$

$$y=\bar{n}_5x+[\mathrm{Cl}^-]_5=10.14934x-0.25027,\ R^2=0.99050 \quad (22)$$

$$y=\bar{n}_6x+[\mathrm{Cl}^-]_6=10.12078x-0.30324,\ R^2=0.98923 \quad (23)$$

As mentioned before, the slope of the line stands for $\bar{n}$ and the intercept stands for $[\mathrm{Cl}^-]$, so the six groups of $\bar{n}$ and $[\mathrm{Cl}^-]$ could be obtained easily. Afterwards, the stability constants of Sb^{5+} with Cl^- could be obtained by Eq. (8), as seen in Eqs. (24)−(29). The value of β increased as the number of ligands increasing, which could concretely reflect the stability of the structure of each complex. Compared to the stability constants of Sb^{3+} with Cl^-, it is easily seen that the values of β of Sb^{5+} with Cl^- were greater than those of Sb^{3+} with Cl^-.

$$\mathrm{Sb}^{5+}+\mathrm{Cl}^-=\mathrm{SbCl}^{4+},\ \lg\beta_1=1.795277456 \quad (24)$$

$$\mathrm{Sb}^{5+}+2\mathrm{Cl}^-=\mathrm{SbCl}_2^{3+},\ \lg\beta_2=3.150053770 \quad (25)$$

$$\mathrm{Sb}^{5+}+3\mathrm{Cl}^-=\mathrm{SbCl}_3^{2+},\ \lg\beta_3=4.191309760 \quad (26)$$

$$\mathrm{Sb}^{5+}+4\mathrm{Cl}^-=\mathrm{SbCl}_4^{+},\ \lg\beta_4=4.954755326 \quad (27)$$

$$\mathrm{Sb}^{5+}+5\mathrm{Cl}^-=\mathrm{SbCl}_5,\ \lg\beta_5=5.427220559 \quad (28)$$

$$\mathrm{Sb}^{5+}+6\mathrm{Cl}^-=\mathrm{SbCl}_6^{-},\ \lg\beta_6=5.511405096 \quad (29)$$

3.3 Presence and distribution of complexes

Besides $\mathrm{SbCl}_i^{(5-i)}$, there existed Sb^{5+}, SbO_3^- ($\mathrm{SbO}_3^-\cdot3\mathrm{H_2O}$ or $\mathrm{Sb(OH)}_6^-$) and $\mathrm{HSbO_3}$ ($\mathrm{HSbO_3\cdot3H_2O}$ or $\mathrm{HSb(OH)_6}$), and the presence and distribution of the antimony compounds in the system could be theoretically studied based on thermodynamic data. The Gibbs free energies of the related compounds are listed in Table 3. The $\Delta_fG_m^\Theta$ of Sb^{5+} could be obtained by using Eq. (28), where the β_5, $\Delta_fG_m^\Theta$ of Cl^- and $\mathrm{SbCl_5(l)}$ are known.

$$\mathrm{Sb}^{5+}+5\mathrm{Cl}^-=\mathrm{SbCl}_5,\ \beta_5=[\mathrm{SbCl}_5]/([\mathrm{Sb}^{5+}][\mathrm{Cl}^-]^5) \quad (30)$$

$$\Delta_rG^\Theta_{\mathrm{m(30)}}=-2.303RT\lg([\mathrm{SbCl}_5]/([\mathrm{Sb}^{5+}][\mathrm{Cl}^-]^5))=-2.303RT\lg\beta_5=\Delta_fG^\Theta_{\mathrm{m(SbCl_5)}}-\Delta_fG^\Theta_{\mathrm{m(Sb^{5+})}}-5\Delta_fG^\Theta_{\mathrm{m(Cl^-)}}$$

$$\Delta_fG^\Theta_{\mathrm{m(Sb^{5+})}}=157.540\ \mathrm{kJ/mol}$$

Similarly, it could be obtained that:

$$\mathrm{Sb}^{5+}+6\mathrm{OH}^-=\mathrm{SbO}_3^-+3\mathrm{H_2O} \quad (31)$$

$$\Delta_rG^\Theta_{\mathrm{m(31)}}=-2.303RT\lg([\mathrm{SbO}_3^-]/([\mathrm{Sb}^{5+}][\mathrm{OH}^-]^6))=\Delta_fG^\Theta_{\mathrm{m(SbO_3^-)}}+3\Delta_fG^\Theta_{\mathrm{m(H_2O)}}-\Delta_fG^\Theta_{\mathrm{m(Sb^{5+})}}-6\Delta_fG^\Theta_{\mathrm{m(OH^-)}}=-439.415\ \mathrm{kJ/mol}$$

Table 3 $\Delta_fG_m^\Theta$ of related compounds [1,15,28]

Species	$\Delta_fG_m^\Theta$/ (kJ·mol^{-1})	Species	$\Delta_fG_m^\Theta$/ (kJ·mol^{-1})
$\mathrm{H_2}$ (g)	0	$\mathrm{Sb_2O_5}$ (s)	−829. 144
$\mathrm{O_2}$ (g)	0	$\mathrm{SbH_3}$ (g)	147.74
$\mathrm{SbO_2^-}$ (aq)	−339.740	$\mathrm{Sb_4O_5Cl_2}$ (s)	−1349.53
$\mathrm{H_2O}$ (l)	−237.141	$\mathrm{Cl^-}$ (aq)	−131.3
$\mathrm{H^+}$ (aq)	0	$\mathrm{SbCl_3}$ (aq)	−323
$\mathrm{OH^-}$ (aq)	−157.293	$\mathrm{SbCl_5}$ (aq)	−529.942
e (aq)	0	HCl (aq)	−131.25
$\mathrm{Sb_2S_3}$ (s)	−140.293	$\mathrm{SbO_3^-}$ (aq)	−514.21
Sb (s)	0	$\mathrm{Sb_2O_3}$ (s)	−626.333
$\mathrm{H_2S}$ (aq)	−27.87	$\mathrm{SO_4^{2-}}$ (aq)	−744.5
$\mathrm{HS^-}$ (aq)	12.05	$\mathrm{HSO_4^-}$ (aq)	−755.9
S (s)	0	$\mathrm{Sb^{3+}}$ (aq)	69.467

As we all know, the concentration of OH^- is a function of pH value:

$$\lg[\mathrm{OH}^-]=\mathrm{pH}-14 \quad (32)$$

The relationship between $[\mathrm{SbO}_3^-]$ and $[\mathrm{Sb}^{5+}]$ is set as

$$[\mathrm{SbO}_3^-]/[\mathrm{Sb}^{5+}]=K_1 \quad (33)$$

Based on Eqs. (31)−(33), K_1 is a function of pH value:

$$\lg K_1=6\mathrm{pH}-7.027403 \quad (34)$$

Furthermore, the relationship between $\mathrm{HSbO_3}$ and Sb^{5+} can be obtained by calculations:

$$\mathrm{HSbO_3}=\mathrm{H}^++\mathrm{SbO}_3^-,\ K_a=10^{-2.73} \quad (35)$$

$$[\mathrm{HSbO_3}]=[\mathrm{H}^+][\mathrm{SbO}_3^-]/K_a=[\mathrm{H}^+]K_1[\mathrm{Sb}^{5+}]/K_a$$

Above all, the concentration of the total antimony ions in the system can be calculated according to Eq. (36):

$$[\mathrm{Sb}^{5+}]_\mathrm{T}=[\mathrm{Sb}^{5+}]+[\mathrm{SbCl}_i^{5-i}]+[\mathrm{SbO}_3^-]+[\mathrm{HSbO_3}] \quad (36)$$

The α_i (α_0, α_1, α_2, α_3, α_4, α_5, α_6, α_7 and α_8) are defined as the percentages of Sb^{5+}, SbCl^{4+}, SbCl_2^{3-}, SbCl_3^{2+}, SbCl_4^+, $\mathrm{SbCl_5(l)}$, SbCl_6^-, SbO_3^- and $\mathrm{HSbO_3}$, which are listed as follows:

$$\begin{aligned}\alpha_0&=[\mathrm{Sb}^{5+}]/[\mathrm{Sb}^{5+}]_\mathrm{T}\\&=[\mathrm{Sb}^{5+}]/([\mathrm{Sb}^{5+}]+[\mathrm{SbCl}_i^{5-i}]+[\mathrm{SbO}_3^-]+[\mathrm{HSbO_3}])\\&=[\mathrm{Sb}^{5+}]/[\mathrm{Sb}^{5+}](1+\beta_1[\mathrm{Cl}^-]+\beta_2[\mathrm{Cl}^-]^2+\beta_3[\mathrm{Cl}^-]^3+\\&\qquad\beta_4[\mathrm{Cl}^-]^4+\beta_5[\mathrm{Cl}^-]^5+\beta_6[\mathrm{Cl}^-]^6+K_1+10^{-\mathrm{pH}}K_1/K_a)\\&=1/(1+\beta_1[\mathrm{Cl}^-]+\beta_2[\mathrm{Cl}^-]^2+\beta_3[\mathrm{Cl}^-]^3+\beta_4[\mathrm{Cl}^-]^4+\\&\qquad\beta_5[\mathrm{Cl}^-]^5+\beta_6[\mathrm{Cl}^-]^6+K_1+10^{-\mathrm{pH}}K_1/K_a)\end{aligned} \quad (37)$$

$$\alpha_i=[\mathrm{SbCl}_i^{5-i}]/[\mathrm{Sb}^{5+}]_\mathrm{T}\ (i=1-6)$$
$$=\beta_i[\mathrm{Cl}^-]^i/(1+\beta_1[\mathrm{Cl}^-]+\beta_2[\mathrm{Sb}^{5+}][\mathrm{Cl}^-]^2+\beta_3[\mathrm{Cl}^-]^3+\beta_4[\mathrm{Cl}^-]^4+\beta_5[\mathrm{Cl}^-]^5+\beta_6[\mathrm{Cl}^-]^6+K_1+10^{-\mathrm{pH}}K_1/K_\mathrm{a}) \quad (38)$$

$$\alpha_7=[\mathrm{SbO}_3^-]/[\mathrm{Sb}^{5+}]_\mathrm{T}$$
$$=K_1/(1+\beta_1[\mathrm{Cl}^-]+\beta_2[\mathrm{Sb}^{5+}][\mathrm{Cl}^-]^2+\beta_3[\mathrm{Cl}^-]^3+\beta_4[\mathrm{Cl}^-]^4+\beta_5[\mathrm{Cl}^-]^5+\beta_6[\mathrm{Cl}^-]^6+K_1+10^{-\mathrm{pH}}K_1/K_\mathrm{a}) \quad (39)$$

$$\alpha_8=[\mathrm{HSbO}_3]/[\mathrm{Sb}^{5+}]_\mathrm{T}$$
$$=10^{-\mathrm{pH}}K_1/K_\mathrm{a}(1+\beta_1[\mathrm{Cl}^-]+\beta_2[\mathrm{Cl}^-]^2+\beta_3[\mathrm{Cl}^-]^3+\beta_4[\mathrm{Cl}^-]^4+\beta_5[\mathrm{Cl}^-]^5+\beta_6[\mathrm{Cl}^-]^6+K_1+10^{-\mathrm{pH}}K_1/K_\mathrm{a}) \quad (40)$$

It can be seen that the presence and distribution of the antimony compounds are functions of the $[\mathrm{Cl}^-]$ and pH values from Eqs. (37)−(40). The α_i changes with different concentrations of Cl^- and pH are plotted in Fig. 7. As shown in Fig. 7, when the pH value was approximately 1.0, there were mainly SbCl_i^{5-i} but not SbO_3^-, HSbO_3 or other pentavalent antimony compounds, which proves that the assumption made in Section 2.2 is correct and the obtained stability constants are credible.

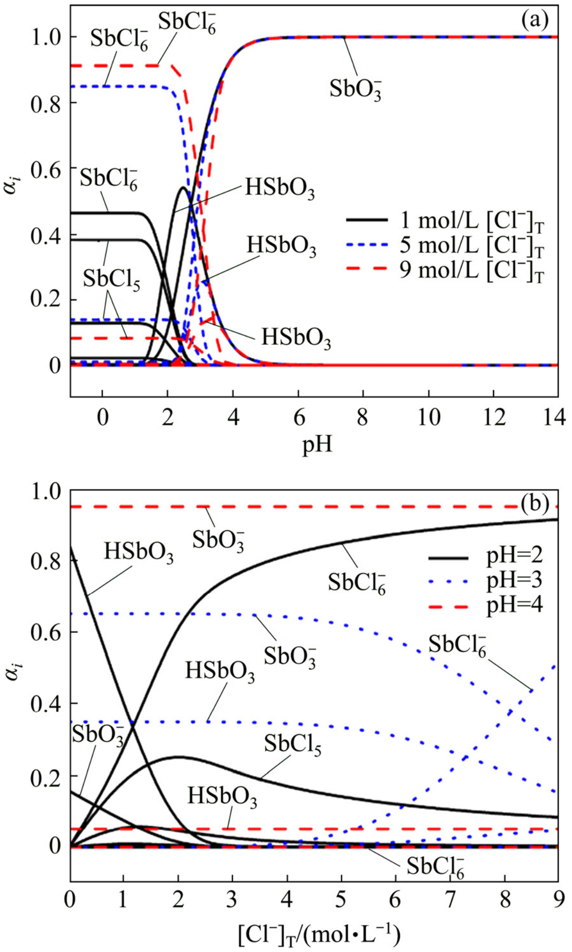

Fig. 7 Distribution of antimony compounds at different pH values (a) and different concentrations of Cl^- (b)

When the pH value was less than 3.0, the antimony was mainly in the form of SbCl_6^- and SbCl_5, and the gap between SbCl_6^- and SbCl_5 increased with the Cl^- concentration increasing. It was because β_6 was greater than β_5, and the increase of Cl^- concentration could strengthen the gap between them. Similarly, the gap between SbCl_6^{3-} and SbCl_5^{2-} in system of Sb^{3+}−Cl^- showed the reverse trend [15], because the β_6 of Sb^{3+} with Cl^- was smaller than the β_5 of Sb^{3+} with Cl^-. The HSbO_3 was distributed in the pH value of 1.0−5.0 with a similar parabola curve, and the α_8 decreased with the Cl^- concentration increasing. The α_7 increased sharply when the pH value was greater than 2.0, and when the pH value was greater than 5.0, the percentage of SbO_3^- was close to 100%.

There were mainly HSbO_3 and SbO_3^- in the solution without Cl^-, as shown in Fig. 7(b). With the increase of pH value, the percentage of HSbO_3 decreased while the percentage of SbO_3^- increased. When the pH value was 2.0, the percentage of SbCl_6^- increased as the Cl^- concentration increased, and the percentages of HSbO_3 and SbO_3^- decreased sharply. The percentage of SbCl_5 increased first, and then decreased when the concentration of Cl^- was more than 2.0 mol/L. As the pH value was 3.0, most HSbO_3 and SbO_3^- were in the solution when the concentration of Cl^- was less than 4.0 mol/L, and the percentage of SbCl_6^- increased when the concentration of Cl^- was more than 4.0 mol/L. When the pH value was 4.0, only HSbO_3 and SbO_3^- were in the solution and there were no changes in the percentages of HSbO_3 and SbO_3^- when the Cl^- concentration changed.

3.4 Thermodynamic study

Because of the complex behavior of Sb with Cl, which has a great influence on the thermodynamic equilibrium of reactions, thermodynamic study was modified by adding the reactions of SbCl_3, SbCl_5, and $\mathrm{Sb}_4\mathrm{O}_5\mathrm{Cl}_2$ into the Sb−S−Cl−$\mathrm{H}_2\mathrm{O}$ system. The thermodynamic data used in this study are listed in Table 3. In this study, the activity coefficient was set to be 1.0, namely, the value of the activity was kept the same with the value of concentration. The calculation procedures were demonstrated in Section 2.3. Thermodynamic equations of the related reactions in the system were calculated under standard conditions, and the results are listed in Table 4.

Table 4 Chemical reactions and equilibrium equations in Sb−S−Cl−H_2O system

No.	Reaction	Equilibrium equation
1	$Sb_2S_3+6H^++6e=2Sb+3H_2S$	$\varphi=-0.098-0.0591pH-0.02955lg[H_2S]$
2	$Sb_2S_3+3H^++6e=2Sb+3HS^-$	$\varphi=-0.305-0.02955pH-0.02955lg[HS^-]$
3	$Sb+3H^++3e=SbH_3$	$\varphi=-0.510-0.0591pH-0.0197lg[SbH_3]$
4	$2Sb_2O_5+10H^++2Cl^-+8e=Sb_4O_5Cl_2+5H_2O$	$\varphi=0.796-0.07388pH+0.00739lg[Cl^-]^2$
5	$Sb_2S_3+6H^++6Cl^-=3H_2S+2SbCl_3$	$pH=-4.318-(1/6)lg([Cl^-]^6/[SbCl_3]^2[H_2S]^3)$
6	$S+2H^++2e=H_2S$	$\varphi=0.144-0.0591pH-0.02955lg[H_2S]$
7	$3S+2SbCl_3+6e=Sb_2S_3+6Cl^-$	$\varphi=0.400-0.00985lg([Cl^-]^6/[SbCl_3]^2)$
8	$6S+Sb_4O_5Cl_2+10H^++12e=2Sb_2S_3+5H_2O+2Cl^-$	$\varphi=0.328-0.04925pH-0.004925lg([Cl^-]^2)$
9	$2SbCl_3+3HSO_4^-+21H^++24e=Sb_2S_3+12H_2O+6Cl^-$	$\varphi=0.350-0.0517pH-0.00246lg([Cl^-]^6/([SbCl_3]^2[HSO_4^-]^3))$
10	$Sb_4O_5Cl_2+6HSO_4^-+52H^++48e=2Sb_2S_3+29H_2O+2Cl^-$	$\varphi=0.332-0.0640pH-0.00123lg([Cl^-]^2/[HSO_4^-]^6)$
11	$Sb_4O_5Cl_2+6SO_4^{2-}+58H^++48e=2Sb_2S_3+29H_2O+2Cl^-$	$\varphi=0.346-0.0714pH-0.00123lg([Cl^-]^2/[SO_4^{2-}]^6)$
12	$Sb_2O_3+3SO_4^{2-}+30H^++24e=Sb_2S_3+15H_2O$	$\varphi=0.362-0.0739pH+0.00246lg([SO_4^{2-}]^3)$
13	$HSO_4^-+7H^++6e=S+4H_2O$	$\varphi=0.333-0.0690pH+0.00985lg[HSO_4^-]$
14	$Sb_4O_5Cl_2+10H^++10Cl^-=4SbCl_3+5H_2O$	$pH=-1.465-0.1lg([SbCl_3]^4/[Cl^-]^{10})$
15	$Sb_2O_5+10H^++10Cl^-=2SbCl_5+5H_2O$	$pH=1.812-0.1lg([SbCl_5]^2/[Cl^-]^{10})$
16	$2SbO_3^-+2H^+=Sb_2O_5+H_2O$	$pH=3.251+0.5lg([SbO_3^-]^2)$
17	$Sb_2O_5+10H^++6Cl^-+4e=2SbCl_3+5H_2O$	$\varphi=0.688-0.14775pH-0.0591lg([SbCl_3]^2/[Cl^-]^6)$
18	$SbCl_5+2e=SbCl_3+2Cl^-$	$\varphi=0.420-0.02955lg([SbCl_3][Cl^-]^2/[SbCl_5])$
19	$HSO_4^-=H^++SO_4^{2-}$	$pH=1.998+lg([SO_4^{2-}]/[HSO_4^-])$
20	$Sb_2O_5+4H^++4e=Sb_2O_3+2H_2O$	$\varphi=0.7034-0.0591pH$
21	$4SbCl_5+8e+5H_2O=Sb_4O_5Cl_2+18Cl^-+10H+$	$\varphi=0.528+0.073875pH-0.007388lg([Cl^-]^{18}/[SbCl_5]^4)$
22	$2Sb_2O_5+8e++2Cl^-+10H^+=Sb_4O_5Cl_2+5H_2O$	$\varphi=0.796-0.073875pH+0.007388lg([Cl^-]^2)$
23	$8e+14H^++4SbO_3^-+2Cl^-=Sb_4O_5Cl_2+7H_2O$	$\varphi=0.892-0.10343pH+0.007388lg([SbO_3^-]^4[Cl^-]^2)$
24	$Sb_4O_5Cl_2+H_2O=2Sb_2O_3+2H^++2Cl^-$	$pH=6.257+0.5lg[Cl^-]^2$
25	$2SbO_3^-+6H^++4e=Sb_2O_3+3H_2O$	$\varphi=0.79957-0.08865pH+0.014775lg([SbO_3^-]^2)$
26	$4e+6H^++2SbO_3^-=Sb_2O_3+3H_2O$	$\varphi=0.799-0.08865pH+0.014775lg([SbO_3^-]^2)$
27	$HS^-+H^+=H_2S$	$pH=6.996-lg([H_2S]/[HS^-])$
28	$2H^++2e=H_2$	$\varphi=-0.0591pH$
29	$O_2+4H^++4e=2H_2O$	$\varphi=1.228-0.0591pH$
30	$ClO_4^-+8H^++8e=Cl^-+4H_2O$	$\varphi=1.389-0.0591pH+0.074lg([ClO_4^-]/[Cl^-])$
31	$H^++Cl^-=HCl$	$pH=lg[Cl^-]-6.30-lg\,p_{HCl}$

It can be seen that there were many equations in the system. Every equilibrium equation could be a line where the potential was set as the *X*-axis and the pH value was set as the *Y*-axis. As shown in the equilibrium equations, the equilibrium states of the antimony compounds would be changed along with the change in potential, pH value, and the activity of related compounds. The potential−pH diagram of the system was plotted in Fig. 8 by integrating the equations in Table 4.

As shown in Fig. 8, the stable regions of the antimony compounds were specific, and the lines between the regions stand for the equilibrium states of the compounds. When the pH value and system potential were satisfied with the conditions of a certain region in the diagram, the antimony would be in the form of the compound in this region, or it could be transformed into this form from other

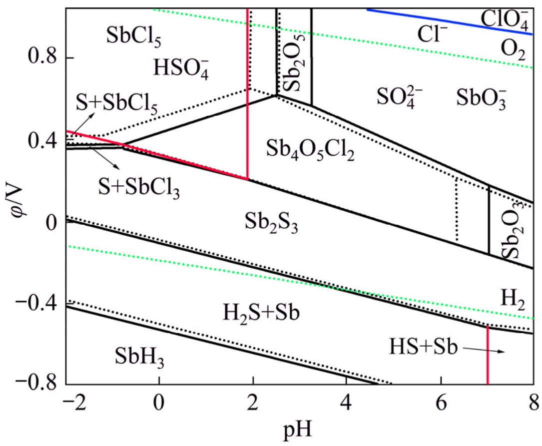

Fig. 8 Potential−pH diagrams of Sb−S−Cl−H$_2$O system (solid lines: Sb 1.0 mol/L, Cl 5.0 mol/L, S 1.5 mol/L; Dotted lines: Sb 0.2 mol/L, Cl 1.0 mol/L, S 0.3 mol/L)

species derived from other regions. Therefore, the experimental conditions could be determined based on the potential−pH diagram. Because SbCl$_5$ in the solution is more stable than Sb^{5+}, the standard redox potential of SbCl$_3$/SbCl$_5$ is lower than that of Sb^{3+}/Sb^{5+}. The gap between the potential of Sb$_2$S$_3$/SbCl$_3$ and SbCl$_3$/SbCl$_5$ is small, and SbCl$_3$ will be oxidized to SbCl$_5$ easily by common oxidants, such as O$_2$, H$_2$O$_2$, Cl$_2$ and NaClO. During the oxidation or reduction processes of antimony hydrometallurgy, the potential of the solution needs to be controlled precisely to prevent the negative influence of the Sb^{3+} and Sb^{5+} compound mixture on production.

4 Conclusions

(1) The stability constants of Sb^{5+} with Cl$^-$ were obtained by theoretical calculation using the absorbance of Sb^{5+}-containing solution, which was detected by spectrophotometry at certain wavelengths of light (380 nm). The 10-based logarithm values for the stability constants were 1.795, 3.150, 4.191, 4.955, 5.427 and 5.511, respectively.

(2) The presence and distribution of pentavalent antimony compounds in the system were studied by theoretical calculations. When the pH value was less than 3.0, the antimony was mainly in the form of SbCl$_6^-$ and SbCl$_5$, and when the pH value was higher than 5.0, the percentage of SbO$_3^-$ was close to 100%. The solution without Cl$^-$ mainly consisted of HSbO$_3$ and SbO$_3^-$.

(3) SbCl$_3$, SbCl$_5$ and Sb$_4$O$_5$Cl$_2$ were considered and calculated in the thermodynamic model of the Sb−S−Cl−H$_2$O system. Thermodynamic study was conducted, and equilibrium equations of the chemical reactions in the system were obtained. The potential−pH diagram was plotted by integrating these equilibrium equations, from which the stable states of the antimony compounds under different conditions were determined.

Acknowledgments

One of the authors, Yun-tao XIN thanks Dr. Li-jun GUO very much for her valuable contributions.

References

[1] ANDERSON C. Antimony production and commodites in SME mineral processing and extractive metallurgy handbook [M]. 2nd ed. Colorado: Society for Mining, Metallurgy and Exploration, 2019.

[2] GUO Zheng-hong, ZHAO li-ping, FANG zheng-ping. The flame retardant and smoke suppression effect of fullerene by trapping radicals in decabromodiphenyl oxide/Sb$_2$O$_3$ flame-retarded high density polyethylene [J]. Fire and Materials, 2017, 41: 916−924.

[3] OUYANG Zhen, LIU shu-fen, TANG Chao-bo, CHEN yi-feng, YE long-gang. Kinetic studies for sulfur-fixing and roasting reduction of antimony sulfide for direct antimony extraction [J]. Vacuum, 2019, 159: 358−366.

[4] RASCHMAN P, SMINČÁKOVÁ E. Kinetics of leaching of stibnite by mixed Na$_2$S and NaOH solutions [J]. Hydrometallurgy, 2012, 113−114: 60−66.

[5] TIAN Qing-hua, WANG heng-li, XIN yun-tao, LI dong, GUO xue-yi. Ozonation leaching of a complex sulfidic antimony ore in hydrochloric acid solution [J]. Hydrometallurgy, 2016, 159: 126−131.

[6] FERNÁNDEZ M A, SEGARRA M, ESPIELL F. Selective leaching of arsenic and antimony contained in the anode slimes from copper refining [J]. Hydrometallurgy, 1996, 41(2−3): 255−267.

[7] YE Long-gang, OUYANG Zhen, CHEN Yong-ming, WANG Heng-hui, XIAO Li, LIU Shu-fen. Selective separation of antimony from a Sb−Fe mixed solution by hydrolysis and application in the hydrometallurgical process of antimony extraction [J]. Separation and Purification Technology, 2019, 228: 115753.

[8] CORBY G Anderson. The metallurgy of antimony [J]. Chemie Der Erde−Geochemistry, 2012, 72: 3−8.

[9] MULTANI R S, FELDMANN T, DEMOPOULOS G P. Antimony in the metallurgical industry: A review of its chemistry and environmental stabilization options [J]. Hydrometallurgy, 2016, 164: 141−153.

[10] ANDERSON C G. Hydrometallurgically treating antimony-bearing industrial wastes [J]. JOM, 2001, 53: 18−20.

[11] HE yun-long, XU rui-dong, HE shi-wei, CHEN han-sen, LI

kuo, ZHU yun, SHEN qing-feng. Alkaline pressure oxidative leaching of bismuth-rich and arsenic-rich lead anode slime [J]. International Journal of Minerals, Metallurgy, and Materials, 2019, 26: 689−700.

[12] RUDNIK E, KOSTĘPSKI M. Comparative studies on the codeposition of antimony and tin from acidic chloride and sulfate-chloride solutions [J]. Archives of Metallurgy and Materials, 2018, 63(2): 709−717.

[13] CHEN Jin-zhong, CAO Hua-zhen, LI Bo, YUAN Hai-jun, ZHENG Guo-qu, YANG Tian-zu. Thermodynamic analysis of separating lead and antimony in chloride system [J]. Transactions of Nonferrous Metals Society of China, 2009, 19: 730−734.

[14] DU xin-ling. Research on the hydrolysis equilibrium of antimony trichloride in the Sb^{3+}−Cl−H_2O system [J]. China Nonferrous Metallurgy, 2012, 41: 75−79. (in Chinese)

[15] TIAN qing-hua, XIN yun-tao, LI yang, WANG xue-hai, GUO xue-yi. Theoretical simulation and experimental study of hydrolysis separation of $SbCl_3$ in complexation−precipitation system [J]. Transactions of Nonferrous Metals Society of China, 2016, 26: 2746−2753.

[16] MAHLANGU T, GUDYANGA F P, SIMBI D J. Reductive leaching of stibnite (Sb_2S_3) flotation concentrate using metallic iron in a hydrochloric acid medium. I: Thermodynamics [J]. Hydrometallurgy, 2006, 84: 192−203.

[17] COSTA L, PAGANETTO G, BERTELLI G, CAMINO G. Thermal decomposition of antimony oxyhalides [J]. Journal of Thermal Analysis, 1990, 36: 1141−1153.

[18] CHEN Xiang-ying, HUH Hyun-sue, LEE S W. Hydrothermal synthesis of antimony oxychloride and oxide nanocrystals: $Sb_4O_5Cl_2$, $Sb_8O_{11}Cl_2$, and Sb_2O_3 [J]. Journal of Solid State Chemistry, 2010, 181(9): 2127−2132.

[19] POURBAIX M, BURBANK J. ATLAS D−Equilibres electrochimiques at 25 °C [M]. Paris: Travaux Réalisés Avec L'appui, 1963.

[20] YANG jian-guang, WU yong-tian. A hydrometallurgical process for the separation and recovery of antimony [J]. Hydrometallurgy, 2014, 143: 68−74.

[21] ROZLOVSKY A A, BONDARENKO E V, DYAKOV V E, ZVONKOV Y F. Method for producing antimony from concentrate: WO Patent, 2004015149 [P]. 2004−02−19.

[22] YANG Fen, ZHANG Xue-jun, TIAN Fang, WU Xu, GAN Fu-xing. Preparation of highly dispersed antimony-doped tin oxide nano-powder via ion-exchange hydrolysis of $SnCl_4$ and $SbCl_3$ and azeotropic drying [J]. Chinese Journal of Aeronautics, 2007, 20(2): 181−186.

[23] KUAN yee-woon, HSU kwang-hsien. Theory of equilibria of complexes in solution. II. The complexity of uranyl thiocyanate by an improved method of corresponding solutions [J]. Acta Chimica Sinica, 1963, 29: 37−43. (in Chinese)

[24] LEWIS J. Modern coordination chemistry [M]. New Jersey: Interscience, 1960.

[25] BRAHM DEVB D J. The applicability of Lambert−Beer's law [J]. Documenta Ophthalmologica, 1974, 38: 279−282.

[26] LI hong-gui. The principles of metallurgy [M]. 2nd ed. Beijing: Science Press, 2005: 174−175. (in Chinese)

[27] STEPHENS P J D, DEVLIN F J C, CHABALOWSKI C F N, FRISCH M J J. Ab initio calculation of vibrational absorption and circular dichroism spectra using density functional force fields [J]. Journal of Physical Chemistry, 1994, 98: 247−257.

[28] CLUGSTON M, FLEMMING R. Advanced chemistry [M]. London: Oxford University Press, 2000.

五价锑离子与氯离子配位稳定常数测定及 Sb−S−Cl−H_2O 体系热力学

李 刚[1]，辛云涛[1]，吕晓东[1]，田庆华[2]，严 康[3]，叶龙刚[4]

1. 重庆大学 材料科学与工程学院，重庆 400044；2. 中南大学 冶金与环境学院，长沙 410083；
3. 江西理工大学 冶金工程学院，赣州 341000；4. 湖南工业大学 冶金与材料工程学院，株洲 412007

摘 要：测定五价锑离子与氯离子的配位常数，并进行 Sb−S−Cl−H_2O 体系的热力学研究。采用分光光度法进行配位稳定常数的测定，在一定波长(380 nm)下测定含五价锑离子溶液在不同氯离子条件下的光度值，通过理论计算得到五价锑离子与氯离子的配位稳定常数。配位稳定常数以 10 为底的对数函数值分别为 1.795、3.150、4.191、4.955、5.427 和 5.511，填补了锑湿法冶金中的部分数据空白。结合配位稳定常数，通过热力学计算研究五价锑离子的赋存形式和分布规律，并将锑离子与氯离子配位行为的影响带入 Sb−S−Cl−H_2O 体系进行热力学研究，得到复合电位−pH 图。

关键词：配位行为；稳定常数；热力学；Sb−S−Cl−H_2O 体系

(Edited by Bing YANG)